Review paper

Immunohistochemistry in placental pathology

Jerzy Stanek

Department of Pathology and Laboratory Medicine, College of Medicine, University of Cincinnati, Cincinnati, United States

Although the clinical background, gross and hematoxylin-eosin examination usually suffice for the placental diagnosis, immunohistochemistry (IHC) is essential in many cases, particularly in high-risk pregnancy. The double E-cadherin/CD34 immunostain is the backbone of it, particularly for diagnosing the early fetal vascular malperfusion (FVM) characterized by the endothelial fragmentation preceding the villous hypovascularity/avascularity of distal FVM. The stain is 3–4 times more sensitive than the stromal vascular karyorrhexis, the other early FVM lesion. The endothelial fragmentation may help in timing FVM and its grading as well as in revealing its temporal heterogeneity. The immunostain makes the FVM the most common pattern of placental injury in the population of pregnancies dominated by mass-forming fetal anomalies. The immunostain is also useful in diagnosing villous hypomaturity by highlighting widened vasculosyncytial membranes. Of other immunostains, cytokeratin IHC is invaluable for confirmation of intrauterine pregnancy in chorionic villi-negative uterine curettings. Cytokeratin and smooth muscle actin are valuable in borderline cases of shallow placental implantation. P57 immunostain is invaluable for the diagnosis of early complete hydatidiform moles. Finally, IHC may be decisive in diagnosing viral placentitis, particularly cytomegaloviral, herpetic and parvoviral.

Key words: placenta, immunohistochemistry, E-cadherin/CD34 immunostain, fetal vascular malperfusion, placental inflammation.

Introduction

Placental examination is regarded as the most valuable and common, albeit retrospective, tool of fetal well-being, compromise or death [1–3] and in the medicolegal practice. In most instances, routine gross examination and histological hematoxylin-eosin staining (HE) together with clinical history is all what is needed to diagnose one of the 4 major patterns of placental injury [4]. However, in a population of high-risk pregnancy/great obstetrical syndromes, abnormal gross placental features or equivocal results of HE pattern, immunohistochemistry (IHC), along with other ancillary tools may be needed. This review is based mainly on the author's many years' experience on the IHC application helpful for the final placental diagnosis, particularly in the fetal vascular malperfusion (FVM).

Confirmation of intrauterine pregnancy

The confirmation or exclusion of the products of conception in biological material may be crucial for confirmation of intrauterine pregnancy, excluding of unsuspected ectopic gestation, and determination of the cause of abortion, particularly in absent fetal somatic tissue, chorionic villi, or obvious trophoblasts on HE staining of the uterine curetting (Figure 1A). The identification of "implantation site decidua" may be useful [2, 5], but frequently is not obvious. The GATA-3 IHC positivity in trophoblasts may be helpful, but lymphocytes are also positive [6]. The cytokeratin IHC shows dispersed spindle/angulated cells against the background of negative decidua (Figure 1B), yielding no false-positive results in cases of ectopic gestation and uterine dysfunctional uterine bleeding. The cytokeratin IHC is particularly useful

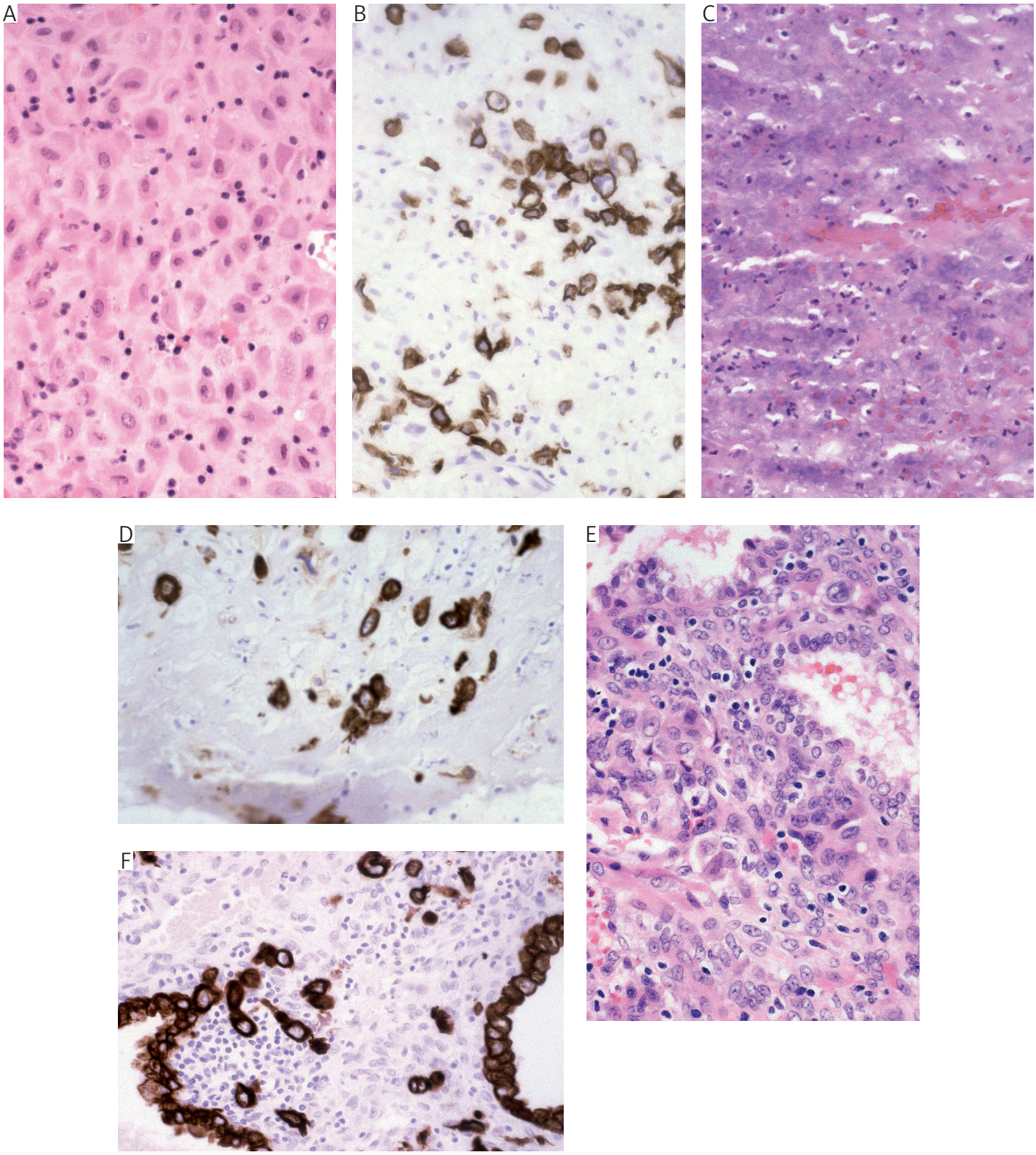

Figure 1. Cytokeratin immunohistochemistry for confirmation of intrauterine pregnancy in chorionic villi-negative early abortion specimens [8] (staining and objective magnifications in parentheses). **A**) Sheets of decidua cells (HE, 50×). **B**) Same block, keratin-positive extravillous trophoblasts against background of negative decidua (low molecular cytokeratin (CAM), 5.2, 50×). **C**) Severe inflammation obscuring cytological details (HE, 50×). **D**) Same block, cytokeratin-positive extravillous trophoblasts against background of negative decidua (CAM 5.2, 50×). **E**) Decidua and endometrial glands (HE, 50×). **F**) In addition to lining of endometrial glands, cytokeratin highlights positive extravillous trophoblasts against background of negative decidua (CAM 5.2, 50×)

when degenerated decidual cells are seen in association with severe inflammation (Figures 1C, D). Even when endometrial glands are present (Figure 1E), they are outlined by the positive cytokeratin but the extravillous trophoblasts are still seen in the decidua (Figure 1F). Isolated positive endometrial cells may be also seen but they are seen lying free outside of the decidua. In exaggerated placental site reaction/placental site nodule, trophoblastic cells will be also positive for cytokeratin [7], as well as human placental lactogen (hPL) and p63 [5], but there is rarely any doubt even on HE staining in such situations. Despite some authors regard cytokeratins, human chorionic gonadotropin and hPL less useful [5], the author's experience is that the cytokeratin immunostain is invaluable, the false negative rate being higher than 20% when HE only is used [8]. In the heterotopic pregnancy, i.e. simultaneous ectopic and intrauterine pregnancies, the trophoblastic cells are seen in the uterine decidua, but such cases are extremely uncommon, and the author observed such coexistence only once in his practice. Neoplastic trophoblasts are positive for SALL-4 IHC in choriocarcinoma, intraplacental choriocarcinoma and in early choriocarcinoma associated with the complete hydatidiform mole [5] but HE staining is decisive in such cases.

Genetic abnormalities

In evaluating pregnancy loss, molar and non-molar villous histologic dysmorphism is taken into consideration, such as clusters of perpendicularly oriented chorionic villi in the chorion leave, stromal and cytotrophoblastic karyomegaly, stromal edema and cavitation, pseudovillous/micronodular cytotrophoblastic proliferation, cytotrophoblastic knots, villous reduced vascularization, villous mineralization and convoluted outlines of chorionic villi with resulting villous stromal trophoblastic pseudoinclusions [1, 5], and villous stromal hypercellularity. As opposed to hypercellularity due to inflammation and increased Hofbauer cells, the mesenchymal hypercellularity of aneuploidies (Figure 2A) may be positive for podoplanin (D240) (pseudolymphatic phenotype, as chorionic villi contain no lymphatics) (Figure 2B) [9, 10]. Stem trophoblastic pseudoinclusions can be mineralized (Figure 2C); they are outlined by E-cadherin (Figure 2D), as opposed to stem thrombi of FVM (see later). The most useful in the differential diagnosis of placental genetic disorders is staining for p57 [11]. In normal chorionic villi, hydropic abortus and partial hydatidiform mole (Figure 2E), villous cytotrophoblasts and stromal cells are positive (Figure 2F) while in early complete hydatidiform mole (Figure 2G) neither (Figure 2H) [2]. In placental mesenchymal dysplasia (PMD) (Figure 2I) only villous cytotrophoblasts are positive (Figure 2J). The caveat is that if PMD coexists with other cytogenetic abnormalities (trisomy, monosomy, triploidy, tetraploidy, duplication/deletion), rare villous stromal cells may also be positive. In difficult cases, other tests (karyotyping, fluorescence *in situ* hybridization, polymerase-chain reaction – PCR, flow cytometry, tests for imprinting, polymorphism microarray) may be needed. Of course, the IHC differential diagnosis is important only in early (1st trimester gestation, early multiple gestation), as in more advanced pregnancies the clinical presentation, fetal malformations and gross examination of the placenta are most helpful. In summary, except for complete hydatidiform moles, placental pathology (including IHC) cannot serve as the only reliable diagnostic tool, but the histological abnormalities can suggest additional testing. Normal placental histology cannot exclude chromosomal abnormalities.

Inflammation

The inflammatory pattern is the most common pattern of placental injury in the second trimester of pregnancy [12], mainly due to the acute chorioamnionitis of the amniotic sac infection syndrome. This is caused by predominantly bacterial or fungal ascending infection, usually requiring no IHC for diagnosis. Ascending herpes simplex virus (HSV) infection is less common (see below) and may require IHC, *in situ* hybridization (ISH), and/or PCR.

Immunohistochemistry plays an important role in diagnosing perinatal viral infections. Cytomegalovirus (CMV) can be devastating for the fetus. In the author's material, placental CMV involvement was associated with the highest perinatal mortality/morbidity [13]. Although in the presence of villous CMV inclusions the diagnosis is easy, IHC (or ISH or PCR) is necessary in the absence thereof and the presence of focal segmental plasmacytic villitis (Figure 3A), pattern of villitis of unknown etiology or even without villitis (Figure 3B) in otherwise unexplainable perinatal death, as about a third of congenital CMV infections show no villitis [13]. Therefore, the combination of the clinical picture and placental pattern of injury creates the best chance to detect congenital CMV infection. Otherwise, unexplained hydrops fetalis may also be caused by congenital CMV infection [14].

Congenital HSV infection may be hematogenous or ascending. The former features patchy necrotizing villitis, commonly without typical viral inclusions in the necrotic villous core (Figure 3C). In such cases the HSV IHC (Figure 3D) as well as ISH and PCR are positive [15]. Similar HE and IHC patterns are seen in congenital varicella-zoster infection [2]. The ascending infection due to maternal uterine cervical HSV inflammation features patchy decidual necrosis or necrosis of amniotic cells [2] positive for HSV IHC

(Figure 3E). It is important that false positivity for HSV IHC may be observed in the epithelial lining of endometrial decidual glands with endogenous biotin accumulation effect mimicking HSV nuclear inclusions on HE staining (Figure 3F) [16] which are positive if biotinylated HSV probes are used (Figure 3G). The use of direct IHC will show full negativity of the gland lining (Figure 3H).

Several placental infections may not evoke characteristic villitis, such as human immunodeficiency

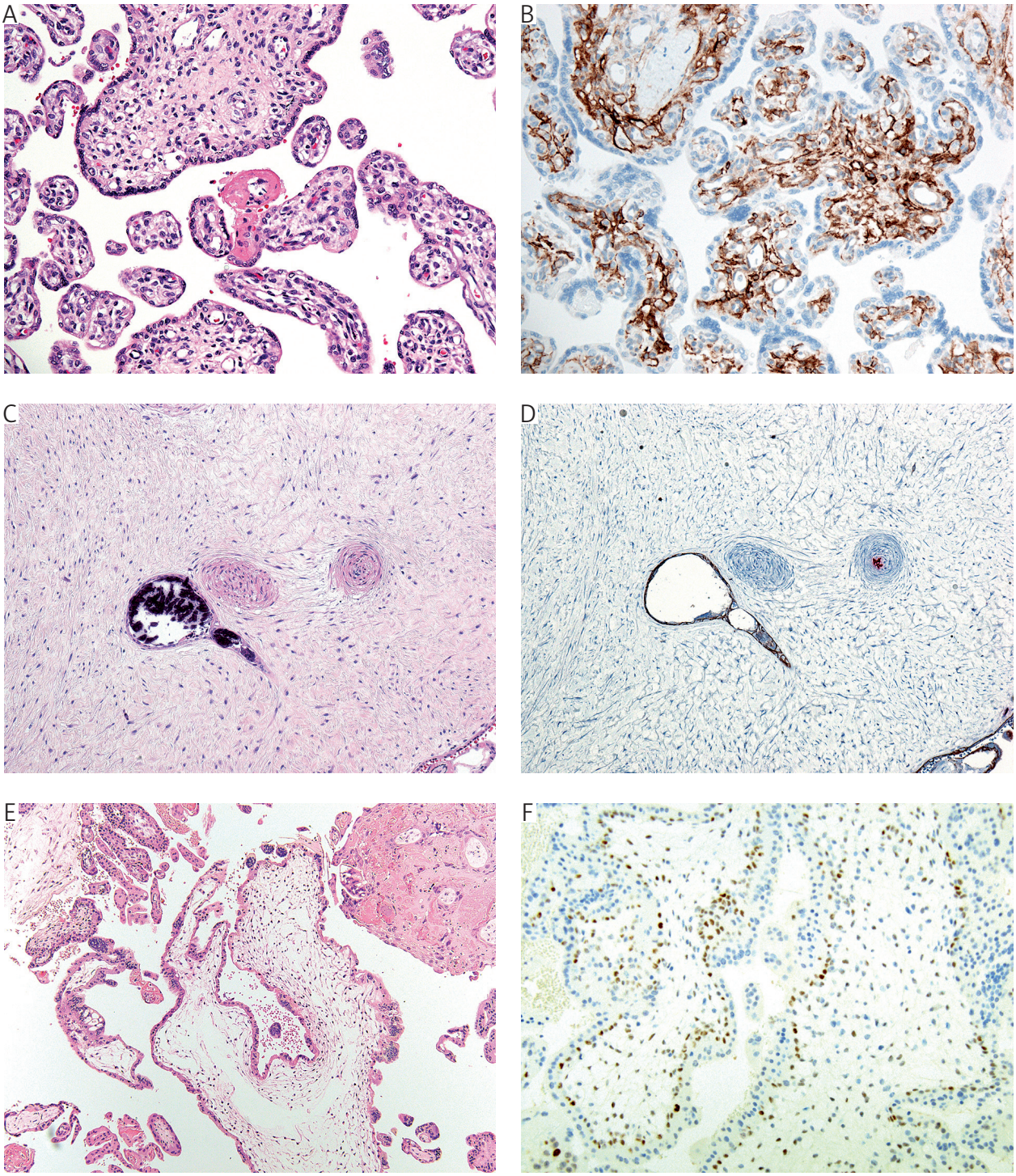

Figure 2. Genetic disorders (staining and objective magnifications in parentheses). **A**) 24 weeks, thick meconium, born en caul, tight nuchal cord 2×, trisomy 18, increased cellularity of distal villi (HE, 20×). **B**) Same case, increased density of stem cells (D240 immunohistochemistry – IHC, 20×). **C**) 38 weeks, mineralized stem trophoblastic pseudoinclusions, myelomeningocele, amniotic band involving umbilical cord (HE, 10×). **D**) Same case, brown rimming of the inclusion (E-cadherin (red)/CD34 (brown) double IHC, 10×). **E**) Early partial hydatidiform mole XXY (HE, 10×). **F**) Same case, IHC positivity in villous cytotrophoblasts and stromal cells, (p 57, 10×)

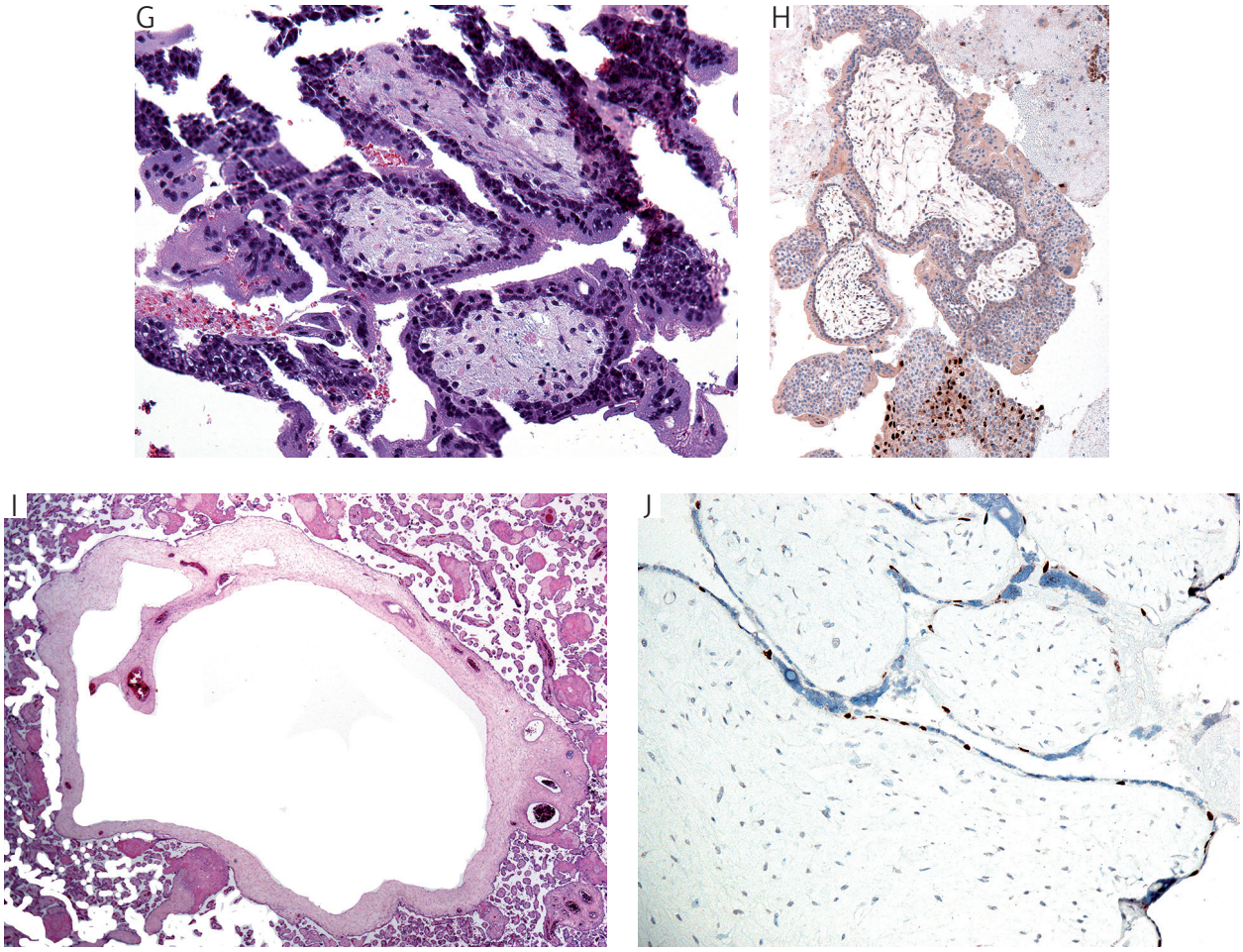

Figure 2. Cont. **G**) Early complete hydatidiform mole (HE, 20×). **H**) Same case, IHC negativity in chorionic villi and positivity in extravillous trophoblasts (positive internal control) (p 57, 10×). **I**) 38 weeks, placental mesenchymal dysplasia (HE, 2×). **J**) Same case, IHC positivity in villous cytotrophoblasts and negativity in villous stromal cells (p57, 20×)

virus (Figure 3I) [13], however with p24 IHC positivity in Hofbauer cells (Figure 3J). The involvement of placenta by syphilis produces non-specific villous enlargement and hypercellularity with most characteristic HE feature being the subacute necrotizing funisitis (Figure 3K), present in only 50% of cases, however [5]. The immunohistochemistry may be positive for treponema pallidum (Figure 3L). The very characteristic intravascular lantern cells of parvovirus B19 infection (Figure 3M) may be confirmed by IHC [5] (Figure 3N), IHC being more sensitive than HE [17]. The COVID-19 infection features the HE triad of massive perivillous fibrinoid deposition (MPFD), villous trophoblastic necrosis, and acute and chronic intervillositis (Figure 3O). All 3 features must be sought as MPFD and chronic histiocytic intervillositis are recurrent in future pregnancies while COVID-19 placentitis is not [5]. The trophoblastic necrosis may be highlighted with complement 9 IHC (Figure 3P), the histiocytic intervillositis with CD163 (Figure 3Q) or CD68, and SARS-CoV-2 IHC positivity is present (Figure 3R) [18, 19]. Of note, villous Hofbauer cell hyperplasia may also occur in Zika viral infection [20].

Hypoxic and abnormal maturation pattens and lesions

Placental histology changes with gestational age. The impact of hypoxia may result in diffuse histological abnormalities that mimic normal physiological histology in other gestational ages. Nevertheless, in most instances, making placental histological diagnosis of diffuse patterns of injury does not need application of IHC. Having said this, placental hypoxic reaction can be seen in the umbilical cord, placental membranes and chorionic plate. Immunohistochemistry may be rarely useful for highlighting necrosis of the media of umbilical arteries (a feature of meconium toxicity) if mild or in the background of the *post* mortem autolytic changes. Complement 9 IHC highlights the necrotic muscle fibers (Figure 4A). In placental membranes, the laminar necrosis (decidual, trophoblastic or mixed) is essentially the membrane infarction, i.e. acute hypoxic lesion, which may require complement 9 IHC for diagnosis if mild or obscured by inflammation (Figure 4B). It may be flanked by caspase 3 or M30 IHC, markers

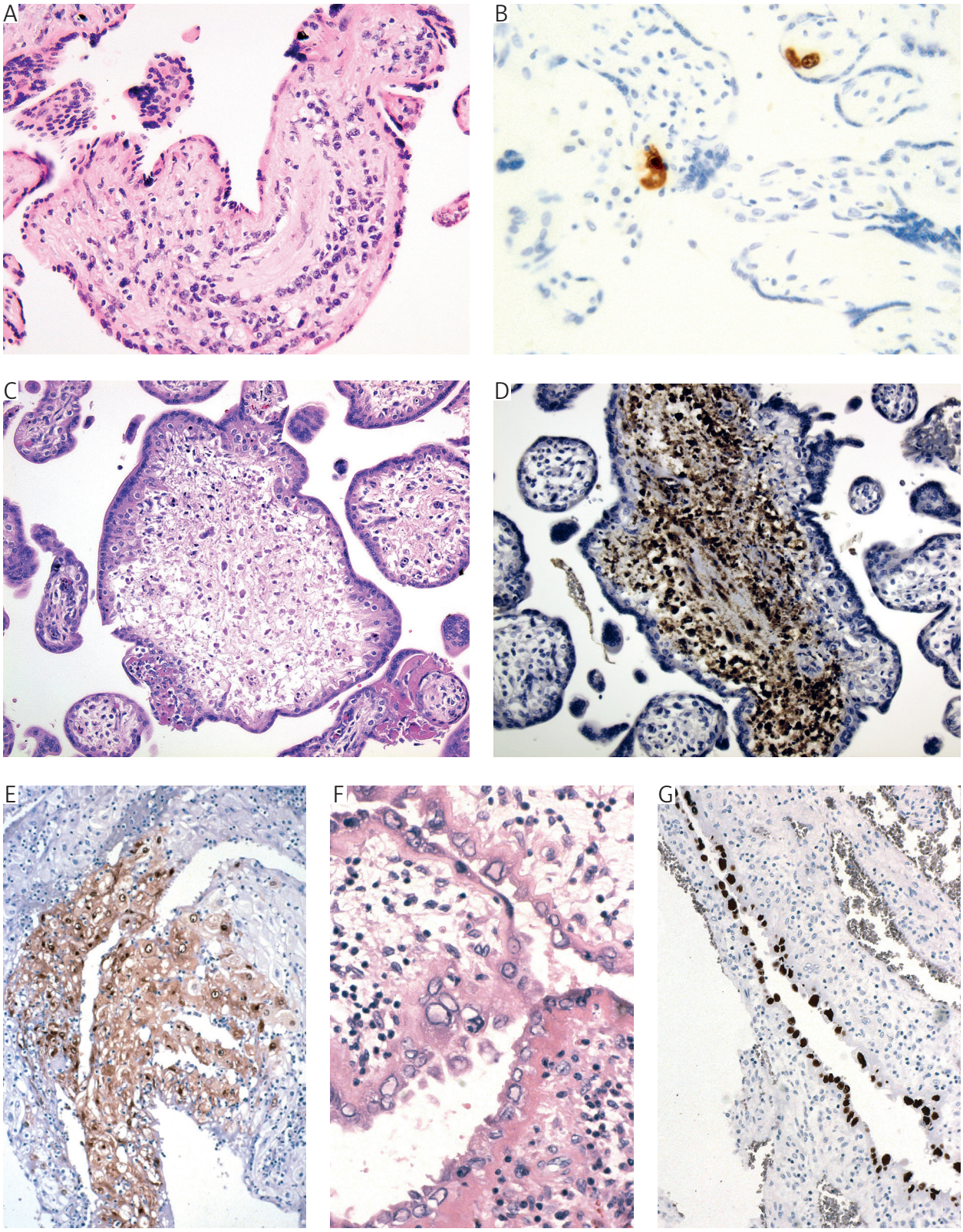

Figure 3. Perinatal infections (staining and objective magnifications in parentheses). A) Plasmacytic villitis, no viral inclusions visible (HE, 40×). B) Same case (CMV immunohistochemistry – IHC, positivity in infected villous core cells, 40×). C) 15 weeks, fetal demise, no herpetic cervical lesions, patchy necrosis of villous cores (HE, 20×). D) IHC positivity of villous core (HSV IHC, 20×). E) 24 weeks, patchy decidual necrosis positive for IHC (HSV IHC, 10×). F) 26 weeks, decidua of maternal floor with glands lining with biotin accumulation effect (HE, 20×). G) Same case, IHC false positivity in lining of decidual glands (HSV IHC, 10×)

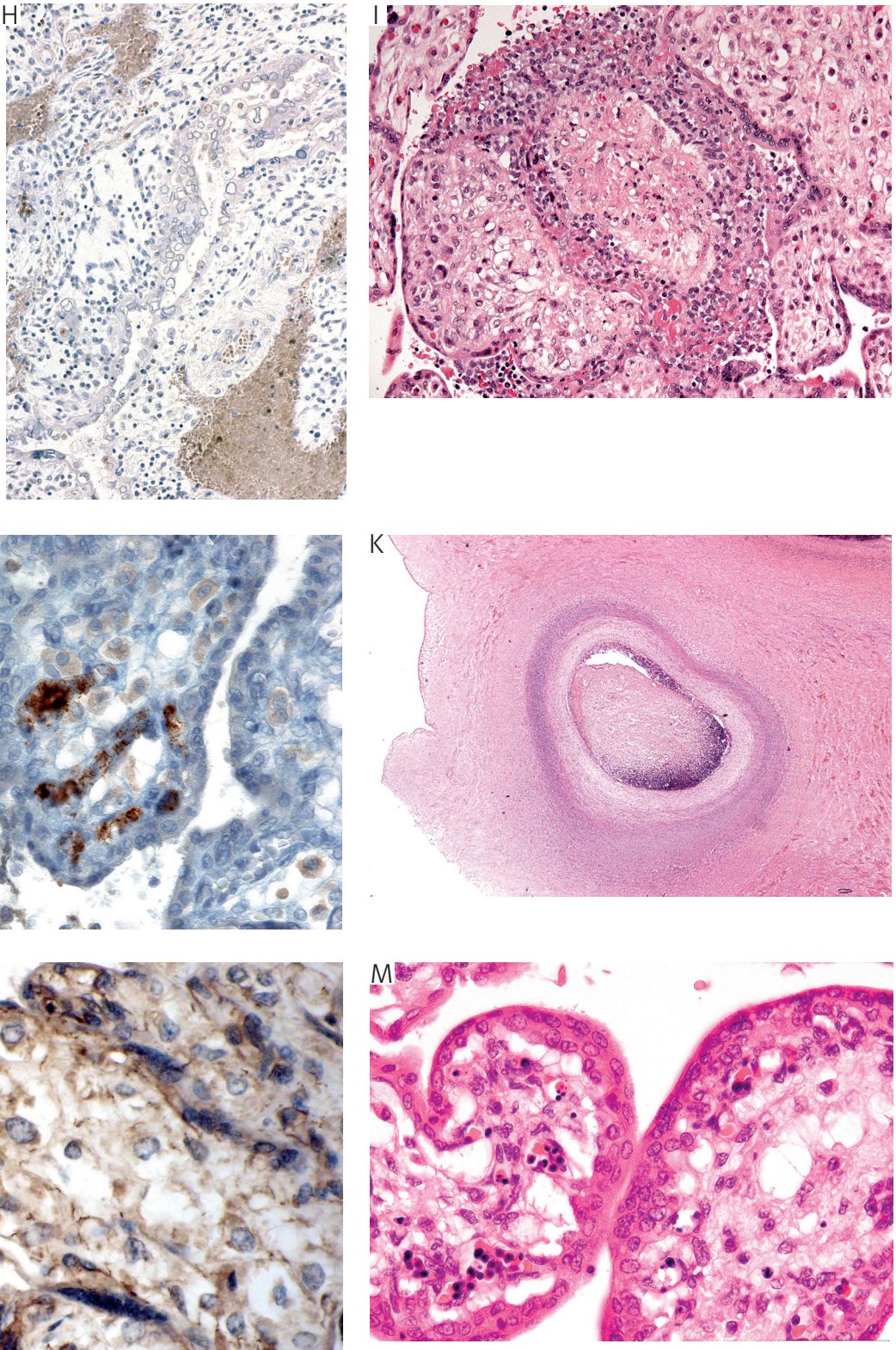

Figure 3. Cont. **H**) Same case, IHC negativity (direct HSV IHC probe, 10×). **I**) 23 weeks, maternal serology positive for HIV, villitis and intervillositis (HE, 20×). **J**) Same case, focal IHC positivity (p24 IHC, 40×). **K**) 32 weeks, subacute necrotizing funisitis (HE, 4×). **L**) Same case, spirochetes positive for HIS in chorionic villus core (Treponema pallidum IHC, 40×). **M**) 25 weeks, hydropic stillbirth, intravascular lantern cells (HE, 60×)

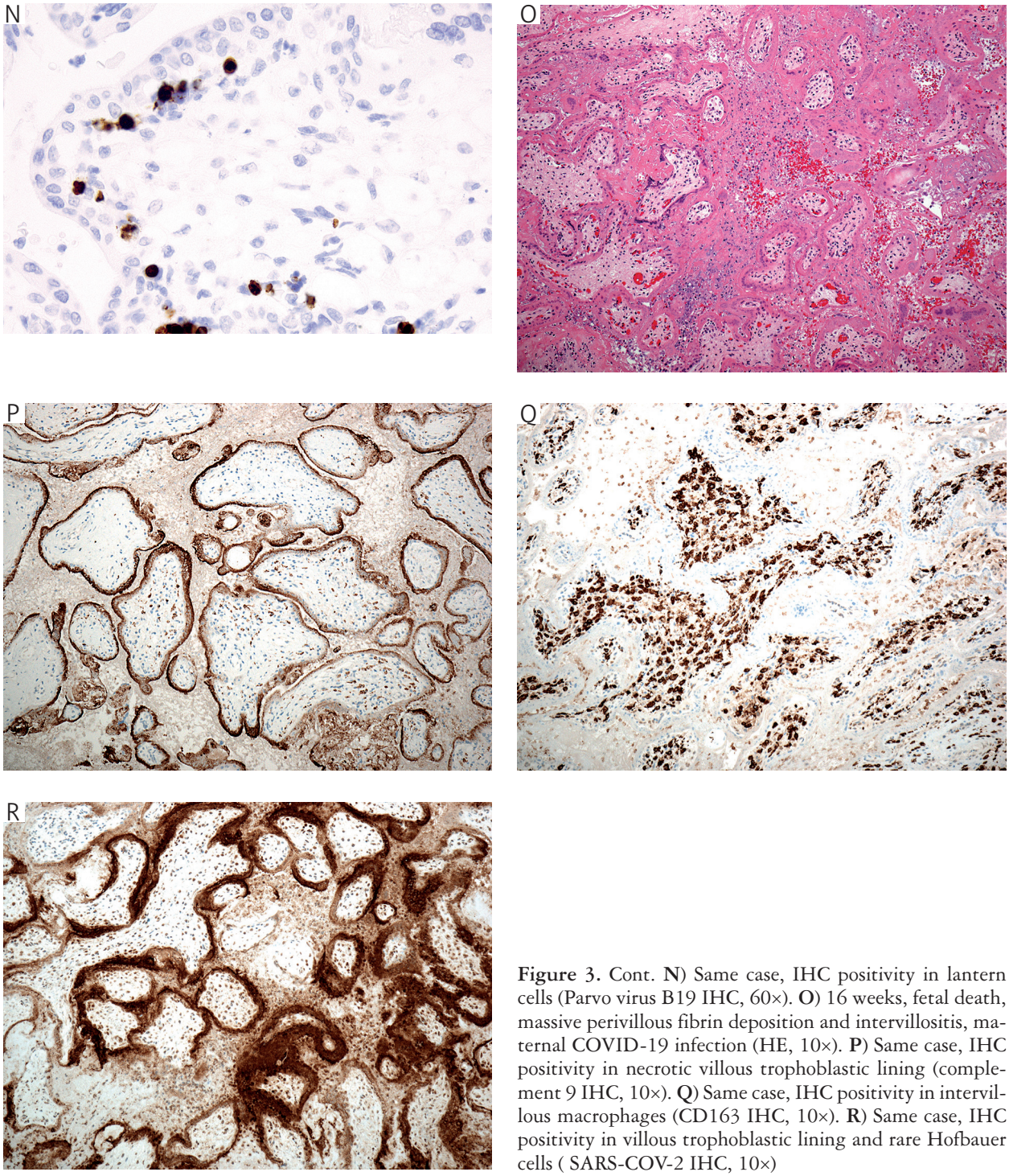

Figure 3. Cont. **N**) Same case, IHC positivity in lantern cells (Parvo virus B19 IHC, 60×). **O**) 16 weeks, fetal death, massive perivillous fibrin deposition and intervillositis, maternal COVID-19 infection (HE, 10×). **P**) Same case, IHC positivity in necrotic villous trophoblastic lining (complement 9 IHC, 10×). **Q**) Same case, IHC positivity in intervillous macrophages (CD163 IHC, 10×). **R**) Same case, IHC positivity in villous trophoblastic lining and rare Hofbauer cells (SARS-COV-2 IHC, 10×)

of irreversible apoptosis, adjacent to positivity for nitrotyrosine residues, a marker of oxidative stress, and for hypoxia-inducible factor 2α [3, 21–23]. Chorionic microcysts/pseudocysts are chronic hypoxic and shallow placentation lesions [3] (see below). They are associated with extravillous trophoblast accumulation in the membranes (defined as the trophoblastic layer thickness of more than 7 cells) [24] that can be highlighted with E-cadherin (Figure 4C), but also with cytokeratins, fascin and CD146 [3]. Diagnosing placental membrane hypoxic lesions increases the sensitivity of placental examination [25].

In the chorionic disc, the abnormal placental histology varies depending on the origin of placental hypoxia (preuterine, uterine or postuterine) [22] with variously abundant and of various mutual proportions of placental structural and cellular components which are gestational-age dependent [3, 12]. All of them can potentially be highlighted with various IHC stains.

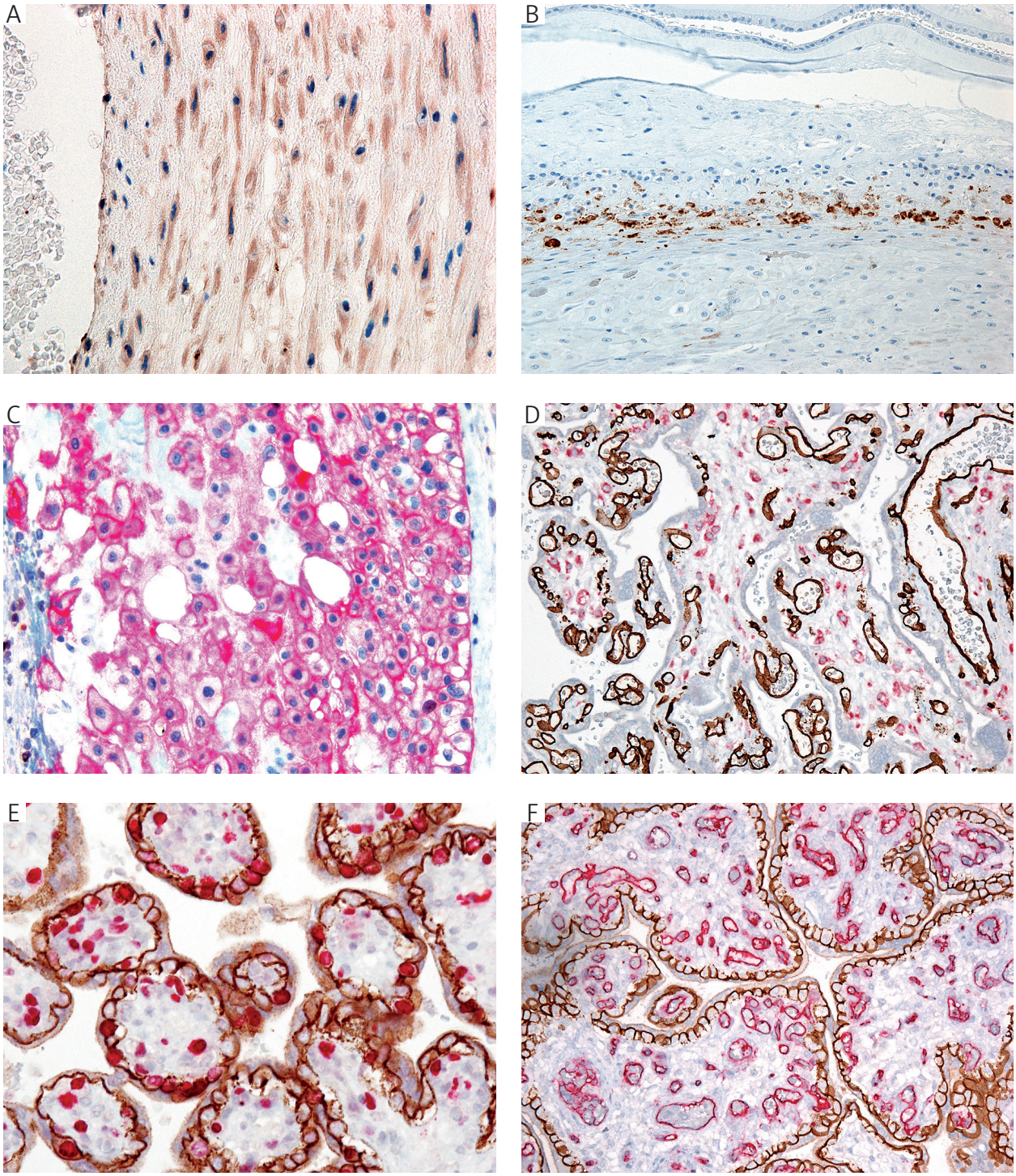

Figure 4. Hypoxic patterns of placental injury (staining and objective magnifications in parentheses). **A**) 40 weeks, stillbirth, true knots of umbilical cord 2×, myonecrosis of umbilical artery (complement 9 immunohistochemistry – IHC, 40×). **B**) 39 weeks, decreased fetal movements, meconium amniotic fluid, brow presentation, neonatal death after 50 minutes, membrane laminar necrosis (complement 9 IHC, 20×). **C**) 31 weeks, placental abruption, increased migratory trophoblasts in placental membranes (E-cadherin IHC, 40×). **D**) 37 weeks, Rh isoimmunization, neonatal depression, horseshoe kidney, tetralogy of Fallot, preuterine hypoxic pattern, double CD68/CD34 IHC highlights increase in villous Hofbauer cells and vascularity (20×). **E**) 41 weeks, early neonatal death, preuterine hypoxic pattern, E-cadherin/CD68 highlighting villous cytotrophoblastic hyperplasia and increased Hofbauer cells (20×). **F**) 28 weeks, gestational diabetes mellitus, with oligohydramnios and multiple congenital anomalies, villous hypomaturity with cytotrophoblastic proliferation, widening of vasculosyncytial membranes and hypervascularity (E-cadherin/CD34 IHC, 20×)

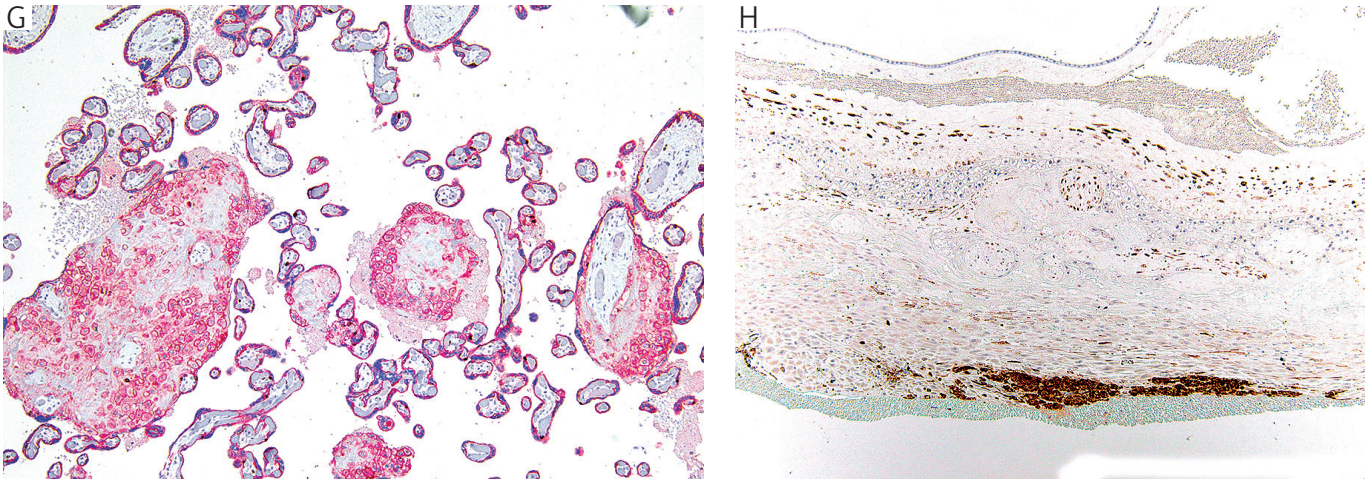

Figure 4. Cont. **G**) 35 weeks, fetal growth restriction, postuterine hypoxic pattern, shallow placental implantation with increased cell islands (E-cadherin, 10×). **H**) 32 weeks, preeclampsia, shallow placental implantation, smooth muscle actin highlights myometrial fibers in placental membranes (10×)

The diffuse villous hypervascularity of the preuterine hypoxic pattern may reach the level of chorangiosis. By CD34 IHC, the numerical threshold of villous capillaries must reach 20 capillaries in distal villi, as opposed to 10 by HE [26]. However, the isolated chorangiosis without other features of diffuse hypoxic change is not prognostically useful unless is associated with other hypoxic cellular abnormalities of the preuterine or uterine hypoxic pattern [27], such as increased Hofbauer cells (Figure 4D), and hyperplasia and/or increased mitotic activity of villous cytotrophoblasts [28] (Figure 4E). The capillaries of chorangiosis and chorangiomatosis are Glut-1 positive, like normal villous capillaries or chorangiomas, unlike true hemangiomas (e.g. of the umbilical cord) which are Glut-1 negative [29]. In addition, chorangiomatosis is a vascular lesion of more proximal villi (stem and intermediate) and is positive for smooth muscle actin (SMA) IHC [5]. In placental dysmaturity (delayed villous maturation) [30], a subtype of the diffuse preuterine hypoxic pattern, the widening of vasculosyncytial membraned is visualized with CD34 IHC [22] or even better with the double E-cadherin/CD34 immunostaining (Figure 4F) [31]. The diagnosis of this pattern is very important as it is seen in poorly controlled maternal diabetes mellitus and pregnancies complicated by otherwise unexplained fetal demise in the third trimester [32].

A distinct category of placental lesions, shallow placental implantation [33], i.e. increased extravillous trophoblasts in placental membranes (Figure 4C) and/or chorionic disc, the latter defined as more than 5 cell islands per placental section [34] (Figure G) and maternal floor are best visualized with a cytokeratin or E-cadherin. Like in placental membranes, more than 7 trophoblast cells on average are diagnostic of shallow placental implantation in the maternal floor [24]. Shallow placental implantation is associated with preeclampsia, decidual arteriolopathy, placental infarction, massive perivillous fibrinoid deposition, and decidual multinucleated trophoblasts [35]. A more controversial feature of shallow placental implantation is basal plate myometrial fibers and occult placenta accreta, a part of the placenta accreta spectrum [36]. In doubtful cases, it may be highlighted with the SMA IHC (Figure 4H). The basal plate myometrial fibers differ from the occult placenta accreta by the presence of cytokeratin (or E-cadherin) positive layer between them and the Rohr fibrinoid (or chorionic villi) [37]. They are associated with thicker layers of implantation site extravillous trophoblasts, stained e.g. with CD146 IHC [38].

In postplacental hypoxia, the accumulation of nitrotyrosine residues, an index of oxidative stress arising from peroxynitrite formation and function, may be highlighted by IHC in the villous endothelium, being associated with increased villous extracellular matrix [39] but is not necessary for diagnosis.

Fetal vascular malperfusion

Originally, the author used the E-cadherin/CD34 double IHC in the differential diagnosis of chronic hypoxic placental injury to assess the vascular syncytial membranes, villous vascularity and density of villous cytotrophoblasts [40]. While doing this, he noticed that the CD34 component of the double immunostaining may highlight the segmental villous hypovascularity/avascularity not easily seen on HE-stained slides and the segmental endothelial fragmentation not seen at all on HE-stained slides. Since then, he started to regard segmental endothelial fragmentation as a lesion of recent FVM filling a gap between normal vascularity to total avascularity, thus complementing stromal vascular karyorrhexis (SVK), which is far less sensitive [41]. It must be mentioned

that the Amsterdam criteria define the FVM placental lesions and grading without the use of IHC, based exclusively on HE examination [3]. Fetal vascular malperfusion is an important pattern of placental injury correlating with perinatal morbidity and mortality [2, 3, 30] but only extensive FVM involving 40–60% of the placental mass is regarded as causative of stillbirth [42].

Large vessels (umbilical cord, chorionic plate and stem) FVM includes fetal vascular ectasia, thrombosis, intramural fibrin deposition, and stem vessel obliteration [30]. Only its multiple lesions (3 or 4) correlate with clinical and placental variables and they may require search for a small distal component unapparent on HE examination. Here is where the double E-cadherin/CD34 immunostain shows the real value as it can upgrade and/or time the FVM [40, 43] (see below). Mineralized stem thrombi (Figure 5A) must be differentiated from the deceptively similar mineralized stem trophoblastic pseudoinclusions (Figure 2C). The former are outlined by the CD34 (Figure 5B) while the latter by the E-cadherin component of the double E-cadherin/CD34 immunostain (Figure 2D). The distinction is important because stem thrombi are lesions of FVM and trophoblastic pseudoinclusions of potential placental aneuploidies [31] (see above).

The distal villous lesions of FVM are clinically more relevant than the proximal large vessel lesions because of longer time needed for their development [44]. By the Amsterdam criteria, distal villous lesions include SVK and clusters of avascular villi [3]. Stromal vascular karyorrhexis is thought to represent FVM of approximately 6–72 hours or more [1], usually 3 days [45]. The CD34 IHC highlights the endothelial fragmentation of recent distal villous FVM 2 days after the thrombotic event (Figure 5C) [45], which is usually not seen on HE-stained slides. This increases the sensitivity of placental examination for FVM [46], can upgrade it, and/or reveal its temporal heterogeneity [47] (Figure 5D), both useful in establishing the cause of perinatal mortality or morbidity and its timing [48]. Although the time of development of SVK partially overlaps with that of endothelial fragmentation by CD34, the latter is 3–4 times less frequent and develops slightly later [49]. If SVK and endothelial fragmentation are adjacent, the endothelial fragmentation areas are usually larger. In most cases, segmental endothelial fragmentation is the only feature of FVM seen on a slide [31]. Diffuse placental endothelial fragmentation is evidence of recent stillbirth [31]. The period for development of avascular villi is 6 days [2], with extensive fibrosis taking 2 or more weeks [1]. In some cases, clusters of sclerotic avascular chorionic villi are better seen on the double IHC than on HE slides (Figure 5D) [31]. However, CD34 can occasionally highlight villous capillaries in even totally sclerotic and avascular villi on HE, thus proving hypovascularity rather than avascularity thereof which can be helpful for timing of distal segmental FVM [50]. The formation of segmental villous mineralization (the remote FVM) requires even more time after vascular occlusion [51], but it will not be discussed here as IHC is not used for its diagnosis. The on-going FVM (coexistence of recent and remote FVM) is most commonly high-grade and associated with preterm birth, stillbirth and fetal growth restriction [48]. This is important because fetal mortality associated with FVM appears to be restricted only to high-grade cases [1], same being true for the short-time neonatal outcome [50]. The temporal heterogeneity of recent and remote lesions of FVM reflects its timing but not etiopathogenesis [47]. The antemortem FVM is also heterogeneous temporally and spatially with the diffuse placental involutional changes [1, 52], and other focal lesions (overlap lesions) [22]. The endothelial fragmentation can be occasionally seen adjacent to other focal placental lesions like infarction (Figure 5E), massive perivillous fibrin deposition (Figure 5F), villous edema (Figure 5G), intervillous thrombus (Figure 5H), as well as villitis of unknown etiology, chorangiomatosis, or foci of avascular villi in fibrin, the significance of such findings being currently unknown [31].

In summary, the double immunostaining was responsible for the FVM being the most common type of placental injury in the author's material dominated by fetal congenital malformations in general, particularly mass-forming, which is likely due to umbilical cord compression [53]. Lesions of FVM rarely occur in isolation in otherwise normal placenta, but frequently coexist with other patterns of placental injury, hypoxic, inflammatory, hyperplastic/neoplastic lesions (overlap lesions) [22, 47]. This may be consequential for the perinatal outcome, as placental vascular thrombosis is a marker for potential systemic fetal/neonatal thrombosis, including brain vascular thrombosis [53]. Routine CD34 IHC made FVM the major pattern of placental injury also in stillbirth [45]. It is even more beneficial in the case of stillbirth than livebirth by highlighting the hypovascular distal villi and/or with endothelial fragmentation, increasing the FVM incidence in stillbirth to 50% [41], making the placental examination an even more powerful tool in explaining the cause of fetal death.

Conclusions

The current review presented the author's experience with using IHC in placental diagnosis (Table I). Although in most routine cases the IHC is not needed, in some instances it is crucial, such as confirmation of pregnancy in chorionic villi-negative uterine curetting, diagnosis of molar pregnancies and PMD in early pregnancy, delayed placental maturation, and FVM. In the latter, the author shared his experience

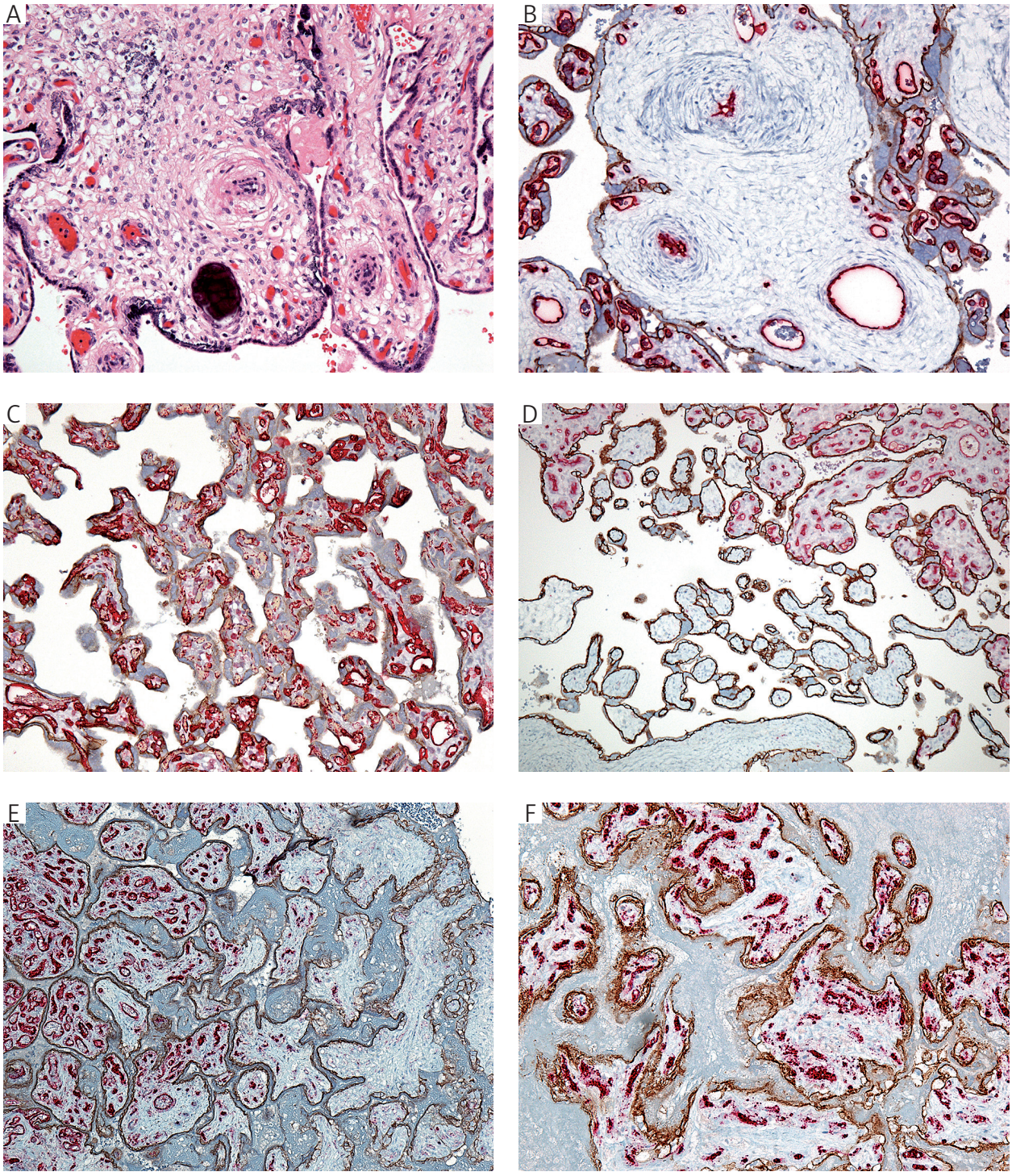

Figure 5. Fetal vascular malperfusion (FVM, objective magnifications in parentheses). **A, B**) 39 weeks, hydrocephaly, absence of septum pellucidum, aqueductal stenosis, absent cerebellar vermis, stem intravascular mineralized thrombi (A, HE). **B**) E cadherin/CD34 immunohistochemistry – IHC, highlights the endothelial lining of thrombosed stem vessel. **C**) 39 weeks, loose nuchal cord, neonatal depression, double outlet right ventricle with D-transposed ductus arteriosus, endothelial fragmentation by E-cadherin/CD34 IHC not seen on HE (20×). **D**) 37 weeks, gestational diabetes mellitus, EXIT to ECMO, neonatal intensive care unit, on heparin, high grade global and segmental FVM with temporal heterogeneity upgraded by E-cadherin (E-cadherin/CD34 IHC, 10×). **E**) 38 weeks, overlap lesion, infarction (right) and FVM (left) by E-cadherin/CD34 IHC (10×). **F**) 31 weeks, maternal anemia and diet-controlled diabetes mellitus, overlap lesion: massive perivillous fibrin deposition and intravillous endothelial fragmentation by E-cadherin/CD34 IHC (20×)

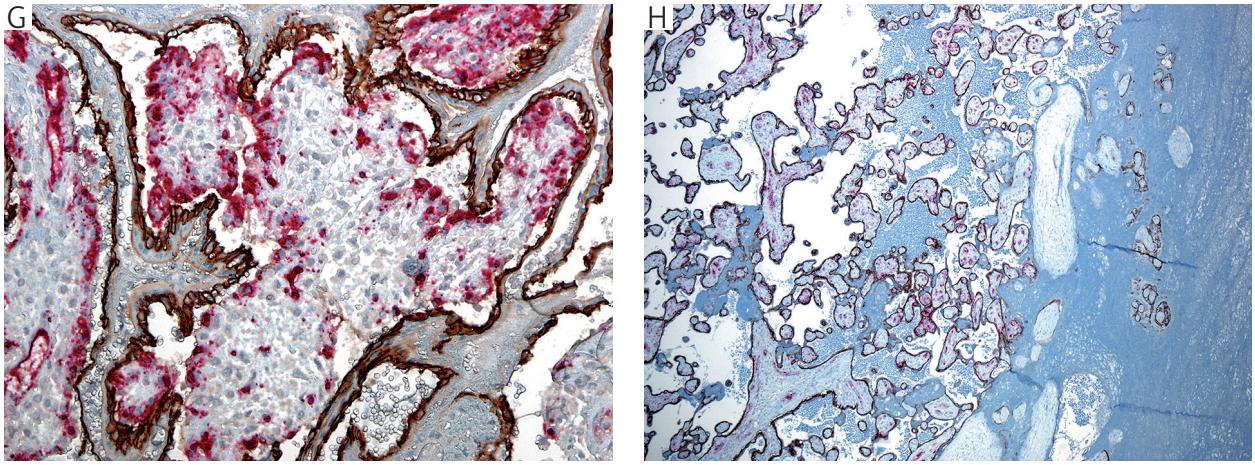

Figure 5. Cont. **G)** 18 weeks, amniotic sac infection syndrome, stillbirth. Overlap lesion: hydropic placenta and FVM with temporal heterogeneity by E-cadherin/CD34 IHC (20×). **H)** 38 weeks, fetal growth restriction, overlap lesion: intervillous thrombus and FVM on-going upgraded by E-cadherin/CD34 immunostain (10×)

Table I. Clinically most important placental immunohistochemistry staining

Area	Test	References
FVM	E-cadherin/CD34	4, 12, 22, 31, 40, 43, 44, 45–51, 53
Confirmation of intrauterine pregnancy in abortion	Cytokeratin, e.g. CAM5.2	7, 8
CMV	CMV IHC	13, 14
HSV	HSV IHC	2, 13, 15
Parvovirus B19	Parvovirus B19 IHC	13, 17
COVID-19	CD163 (68), Complement 9, Covid19-SARS IHC	5, 18–20
HIV	P24 IHC	13
Zika	CD68 CD163	20
Chronic histiocytic intervillositis	CD68	1
Syphilis	Treponema pallidum IHC	13
Complete hydatidiform mole	P57 IHC	1, 2
Placental mesenchymal dysplasia	P57 IHC	11
Villous stromal stem cell hyperplasia	Podoplanin (D240) IHC	10
Delayed villous maturation/villous dysmaturity	E-cadherin/CD34	31
Maternal vascular malperfusion, chronic	E-cadherin/CD34	22, 28, 30
Villous cytotrophoblastic hyperplasia	E-cadherin	2, 22, 31
Villous hypervascularity	CD34 IHC	22, 26, 27
Hofbauer cells hyperplasia	CD68 IHC	1
Cord meconium myonecrosis	Complement 9 IHC	1
Laminar decidual necrosis	Complement 9 IHC	23
Shallow placental implantation	E-cadherin, cytokeratins, CD146	24, 33, 34
Occult placenta accreta, membrane and maternal floor myofibers	Smooth muscle actin	37, 38

CMV – cytomegalovirus, FVM – fetal vascular malperfusion, HSV – herpes simplex virus, IHC – immunohistochemistry

with his preferred double E-cadherin/CD34 immunostain. The staining turned out to be a very useful tool in the diagnosis of distal villous lesions of FVM, particularly early, its grading and timing. It increases the sensitivity of placental diagnosis of FVM. The author routinely performs the stain on a grossly unremarkable placental section in the population of placentas from pregnancies abundant with congenital malformations, particularly mass-forming, with possible umbilical cord compromise and aneuploidies. It increases the sensitivity of placental examination for FVM, can upgrade it and reveal its temporal heterogeneity, thus helping in diagnosis of a cause and timing of fetal injury. The author strongly encourages its use by all placentologists.

Disclosures

1. Institutional review board statement: Not applicable.
2. Assistance with the article: None.
3. Financial support and sponsorship: None.
4. Conflicts of interest: None.

References

1. Roberts DJ, Polizzano C. Atlas of placental pathology. American Registry of Pathology, Arlington, Virginia 2021.
2. Heerema-McKenney A, Popek EJ, DePaepe ME (eds). 2nd ed. Diagnostic pathology: placenta. Amirsys, Elsevier, Philadelphia 2019.
3. Khong TY, Mooney EE, Nikkels PGJ, Morgan TK, Gordijn SJ (eds). Pathology of the placenta, Springer 2019, 83.
4. Redline RW, Ravishankar S, Bagby CM, Saab ST, Zarei S. Four major patterns of placental injury: a stepwise guide for understanding and implementing the 2016 Amsterdam consensus. Modern Pathol 2021; 34: 1074-1092.
5. Kim CF, Ravishankar S, Sybenga AB. Survival guide to placental pathology. Roberts D (ed.). The Innovative Science Press, Arlington, VA, USA 2026.
6. Horn LC, Opitz S, Handzel R, Brambs CE. Histopathology and clinical aspects of extrauterine pregnancy. Pathologe 2018; 39: 431-444.
7. Daya D, Sabet L. The use of cytokeratin as a sensitive and reliable marker for trophoblastic tissue. Am J Clin Pathol 199; 95: 137-141.
8. Konoplev SN, Dimashkieh, HH, Stanek J. Cytokeratin immunohistochemistry: a procedure for exclusion of pregnancy in chorionic villi-negative specimen. Placenta 2004; 25: 146-152.
9. Castro E, Tony Parks W, Galambos C. Neither normal nor diseased placentas contain lymphatic vessels. Placenta 2011; 32: 310-316.
10. Wang Y, Sun J, Gu Y, Zhao S, Groome LJ, Alexander JS. D2-40/podoplanin expression in human placenta. Placenta 2011; 32: 27-32.
11. Faye-Petersen OM, Kapur RP. Placental mesenchymal dysplasia. Surg Pathol Clin 2013; 6: 127-151.
12. Stanek J, Funk D. Clinicopathologic correlations and interdependence of basic patterns of placental injury. Virchows Arch 2025; 487: 1357-1370.
13. Stanek J. Placental infectious villitis versus villitis of unknown etiology. Pol J Pathol 2017; 68: 55-65.
14. Sampath V, Narendran V, Donovan EF, Stanek J, Schleiss MR. Nonimmune hydrops fetalis due to congenital cytomegalovirus infection in a premature infant. J Perinatol 2005; 25: 608-611.
15. Bedolla G, Stanek J. Intrauterine hematogenous herpetic infection. Arch Pathol Lab Med 2004; 128: 1189-90.
16. Bussolati G, Leonardo E. Technical pitfalls potentially affecting diagnoses in immunohistochemistry. J Clin Pathol 2008; 61: 1184-1192.
17. Li JJ, Henwood T, Hal SV, Charlton A. Parvovirus infection: an immunohistochemical study using fetal and placental tissue. Ped Dev Pathol 2025; 18: 30-39.
18. Sharps MC, Hayes DJL, Lee S, Zou Z, Brady CA, Almoghrabi Y, et al. A structural review of placental morphology and histopathological lesions associated with SARS-CoV-2 infection. Placenta 2020; 101: 13-29.
19. Marton T, Hargitai B, Hunter K, Pugh M, Murray P. Massive perivillous fibrin deposition and chronic histiocytic intervillosits a complication of SARS-CoV-2 infection. Pediatr Dev Pathol 2021; 24: 450-454.
20. Rosenberg AZ, Yu W, Hill DA, Reyes CA, Schwartz DA. Placental pathology of Zika virus: viral Infection of the placenta Induces villous stromal macrophage (Hofbauer cell) proliferation and hyperplasia. Arch Pathol Lab Med 2017; 141: 43-48.
21. Kadyrov M, Kaufmann P, Huppertz B. Expression of a cytokeratin 18 neo-epitope is a specific marker for trophoblast apoptosis in human placenta. Placenta 2001; 22: 44-48.
22. Stanek J. Hypoxic patterns of placental injury: a review. Arch Pathol Lab Med 2013; 137: 706-720.
23. Stanek J, Al-Ahmadie H. Laminar necrosis of placental membranes: a histologic sign of uteroplacental hypoxia. Pediatr Dev Pathol 2005; 8: 34-42.
24. Stanek J. Membrane microscopic chorionic pseudocysts are associated with increased amount of placental extravillous trophoblasts. Pathology 2010; 42: 125-130.
25. Stanek J. Diagnosing placental membrane hypoxic lesions increases the sensitivity of placental examination. Arch Pathol Lab Med 2010; 134: 989-995.
26. Mutema G, Stanek J. Numerical criteria for the diagnosis of placental chorangiosis using CD34 immunostaining. Trophoblast Res 1999; 13: 443-452.
27. Stanek J. Chorangiosis of chorionic villi: what does it really mean? Arch Pathol Lab Med 2016; 140: 588-593.
28. Kingdom JC, Kaufmann P. Oxygen and placental villous development: origins of fetal hypoxia. Placenta 1997; 18: 613-621.
29. Ferreira EO, Stefanovici C, Kostadinov S, Duncan V. Umbilical cord hemangiomas: a multi-institutional case series with literature review. Pediatr Dev Pathol 2024; 27: 569-575.
30. Khong TY, Mooney EE, Ariel I, Balmus NCM, Boyd TK, Brundler MA, et al. Sampling and definitions of placental lesions. Amsterdam placental workshop group consensus statement. Arch Pathol Lab Med 2016; 140: 698-713.
31. Stanek J. E-cadherin/CD34 double immunostain in placental diagnosis. Pol J Pathol 2024; 75: 171-181.
32. Higgins M, McAuliffe FM, Mooney EE. Clinical associations with a placental diagnosis of delayed villous maturation: a retrospective study. Pediatr Dev Pathol 2011; 14: 273-279.
33. Stanek J. Shallow placentation: A distinct category of placental lesions. Am J Perinatol 2023; 40: 1328-1335.
34. Stanek J. Chorionic disc extravillous trophoblasts in placental diagnosis. Am J Clin Pathol 2011; 136: 540-547.
35. Stanek J, Weng E. Microscopic chorionic pseudocysts in placental membranes: a histologic lesion of in utero hypoxia. Pediatr Dev Pathol 2007; 10: 192-198.
36. Bonanni G, Lopez-Giron MC, Allen L, Fox K, Silver RM, Hobson SR, et al. Guidelines on placenta accreta spectrum disorders; a systematic review. Obstet Gynaecol Surv 2026; 81: 10-12.

37. Stanek J. Placenta creta: a spectrum of lesions associated with shallow placental implantation. Obstet Gynecol Int 2020; 2020: 4230451.
38. Stanek J, Drummond Z. Occult placenta accreta: the missing link in the diagnosis of abnormal placentation. Pediatr Dev Pathol 2007; 10: 266-262.
39. Stanek J, Eis ALW, Myatt L. Nitrotyrosine immunostaining correlates with increased extracellular matrix: evidence of post-placental hypoxia. Placenta 2001; 22: S56-S62.
40. Stanek J. Fetal vascular malperfusion. Arch Pathol Lab Med 2018; 142: 679-680.
41. Stanek J, Abdaljaleel M. CD34 immunostain increases the sensitivity of placental diagnosis of fetal vascular malperfusion in stillbirth. Placenta 2019; 77: 30-38.
42. Pinar H, Carpenter M. Placenta and umbilical cord abnormalities seen with stillbirth. Clin Obstet Gynecol 2010; 53: 656-672.
43. Stanek J. Clinical significance of the large fetal vessel lesions in placental fetal vascular malperfusion. Lab Invest 2024; 104: 102089.
44. Stanek J. Distal villous lesions are clinically more relevant than proximal large muscular vessel lesions of placental fetal vascular malperfusion. Histol Histopathol 2022; 37: 365-372.
45. Stanek J, Drach A. Placental CD34 immunohistochemistry in fetal vascular malperfusion in stillbirth. J Obstet Gynaecol Res 2022; 48: 719-728.
46. Stanek J. Placental recent/on-going foetal vascular malperfusion with endothelial fragmentation is diagnostically equivalent to established distal villous lesions of foetal vascular malperfusion. Pol J Pathol 2022; 73: 198-207.
47. Stanek J. Temporal heterogeneity of placental segmental fetal vascular malperfusion: timing but not etiopathogenesis. Virchows Arch 2021; 478: 905-9214
48. Stanek J. Timing of histological distal villous fetal vascular malperfusion in the placenta: clinical significance and placental features. Ann Clin Lab Sci 2024; 54: 289-298.
49. Stanek J. CD34 immunostain increases the sensitivity of placental examination for distal villous vascular malperfusion in livebortn infants. Placenta 2023; 140: 117-124.
50. Stanek J. Grading fetal vascular malperfusion and short-term perinatal outcome. Pol J Pathol 2020; 71: 291-300.
51. Stanek J. Segmental villous mineralization: a placental feature of fetal vascular malperfusion. Placenta 2019; 86: 20-27.
52. Genest DR. Estimating the time of death in stillborn foetuses: II. Histologic evaluation of the placenta; a study of 71 stillborns. Obstet Gynecol 1992; 80: 585-592.
53. Stanek J. Placental fetal vascular malperfusion in maternal diabetes mellitus. J Perinat Med 2024; 53: 179-187.

Address for correspondence

Professor Jerzy Stanek, Md, PhD
Department of Pathology and Laboratory Medicine
College of Medicine
University of Cincinnati
Cincinnati, United States
e-mail: stanekjw@ucmail.uc.edu